ELSEVIER

Thermochimica Acta 314 (1998) 213–227

thermochimica acta

Excess enthalpies and phase equilibria in the Pb–Sb–Te system

Andreas Schlieper[1], Frank Römermann, Roger Blachnik*

Anorganische Chemie, Universität Osnabrück, Postfach 44 69, D-49069 Osnabrück, Germany

Received 29 September 1997; accepted 14 October 1997

Abstract

The excess enthalpies of liquid binary Sb–Te alloys and of the ternary Pb–Sb–Te system were determined in a heat-flow calorimeter along the sections Pb_ySb_{1-y}–Te with y=0.2, 0.5 and 0.8 at 1173 K and with y=0.5 at 1073 K. The largest values of the exothermic enthalpies are found on a line stretching from PbTe to Sb_2Te_3. The association model with additional ternary interaction parameters was applied for the analytical description of the ternary melt. In addition, the phase equilibria were determined by DTA and X-ray diffraction measurements. The thermodynamic functions of the quasi-binary sections PbTe–Sb and PbTe–Sb_2Te_3 were optimized and the phase equilibria calculated. © 1998 Elsevier Science B.V.

Keywords: Enthalpies of mixing of Pb–Sb–Te; Enthalpies of mixing of Sb–Te; Phase diagram Pb–Sb–Te; Section PbTe–Sb; Section PbTe–Sb_2Te_3

1. Introduction

The excess enthalpies in liquid-metal–tellurium alloys often vary as triangular-shaped functions of the concentration with exothermic minima close to the composition of a congruent melting compound in the system. According to Wagner [1], this unusual behaviour can be explained by the formation of stoichiometric associates in the liquid state due to electron transfer from the metal to the chalcogen or formation of covalent bonds between these elements.

Within the scope of systematic investigations of the excess enthalpies in ternary systems, we have now measured the excess enthalpies of Sb–Te and Pb–Sb–Te alloys in the liquid state. The association model was used to describe the thermodynamic functions of the melt. For preliminary clarification of the liquidus surface in the ternary system and phase equilibria on the quasi-binary sections PbTe–Sb and PbTe–Sb_2Te_3, we performed DTA and X-ray diffraction measurements. An optimized set of thermodynamic functions for the quasi-binary sections was obtained from experimental data by a computer operated least-squares method.

2. Experimental

2.1. Calorimetric measurements

The measurements were performed with a high-temperature heat flow calorimeter [2] along three cross sections Pb_ySb_{1-y}–Te. The measurements started with the liquid binary Pb_ySb_{1-y} alloys, with

*Corresponding author. Fax: +49-541/969-2370; e-mail: blachnik@physik.uni-osnabrueck.de

[1]Present address: Brandenburgische Technische Universität Cottbus, Lehrstuhl Anorganische Chemie, Karl-Marx-Str. 17, 03044 Cottbus, Germany.

PII S0040-6031(97)00468-1

y=0.2, 0.5 and 0.8 at T=1173 K and with y=0.5 at 1073 K. Small amounts of tellurium (T=298 K) were consecutively added to this melt. On the tellurium-rich side of the sections, the measurements started with pure liquid Te and small amounts of the binary Pb_ySb_{1-y} (T=298 K) alloy were successively added. The enthalpy increments, $H(T)$–H(298 K), of Pb_ySb_{1-y} and Te were determined in separate experiments. The calibration of the calorimeter was carried out before and after each mixing experiment by dropping Sn (T=298 K) into a second tube, the end of which was located in the melt. The enthalpy increments of tin were taken from Barin [3]. The reproducibility was better than ±3%. All experiments were carried out under dry argon gas at atmospheric pressure.

2.2. Phase diagram investigations

The liquidus surface of the ternary Pb–Sb–Te system and the quasi-binary sections PbTe–Sb and PbTe–Sb_2Te_3 were experimentally determined. The identification of the phases was carried out with the aid of an X-ray diffractometer (STOE automated diffractometer system, $\lambda_{Cu,K\alpha}$=154.056 pm). DTA measurements were performed at a heating rate of 10 K min^{-1}, using a self-constructed DTA with Si as reference and a NEWTRONIC furnace, Model Micro 96 whose main characteristics have already been described [4]. The samples were prepared in the desired compositions from the pure elements (Pb, Preussag, 99.999%; Sb, Preussag, 99.999%; Te, Preussag, 99.999%) and placed in silica tubes; in addition samples with the composition of the ternary compound $Pb_2Sb_6Te_{11}$, described by Abrikosov et al. [5,6]. The evacuated and sealed tubes were heated to a temperature well above the melting temperature and vigorously shaken. After quenching, the alloys were annealed for 4500 h at different temperatures below the solidus line, and at 723 and 623 K for $Pb_2Sb_6Te_{11}$.

3. Analytical description

3.1. Binary systems

The analytical description of the thermodynamic functions for the liquid alloys was carried out by means of the association model [7]. Based on this concept, the formation of short-range ordered associates A_iB_j in the melt is assumed, which have a well-defined stoichiometry corresponding to the composition of a congruent melting compound in the solid state. A system of three different species is thus obtained with n_A and n_B moles of free atoms A and B in equilibrium with $n_{A_iB_j}$ moles of associates. The mass action law with an association constant $K_{A_iB_j}$ can be applied to the reaction

$$iA + jB \leftrightarrow A_iB_j.$$

The thermodynamic functions of the melt can be described by the parameters $\Delta H^0_{A_iB_j}$ and $\Delta S^0_{A_iB_j}$, respectively, the enthalpy and entropy of formation of the associates and $C^G_{X,Y}$ the interaction parameter between two species X and Y, with $C^G_{X,Y} = C^H_{X,Y} - TC^S_{X,Y}$ [8]. These coefficients required for the calculation of the limiting binaries, were derived by the aid of the program 'BINGSS' developed by Lukas et al. [9,10].

3.2. Ternary systems

If in a ternary system one associate in each binary system is formed, three such equilibria have to be considered. Without the formation of ternary associates, six additional interaction parameters may then be needed for the analytical description of the liquid ternary system: the interactions between an associate of a binary system and the third pure component, C^H_{C,A_iB_j}, C^H_{B,A_kC_l} and C^H_{A,B_uC_v}, and between two different binary associates, $C^H_{A_iB_j,A_kC_l}$, $C^H_{A_iB_j,B_uC_v}$ and $C^H_{A_kC_l,B_uC_v}$ [8].

3.3. Quasi-binary sections

The thermodynamic functions of a quasi-binary section can be expressed by Redlich–Kister polynomials [11] in order to calculate the phase equilibria [12]. The excess term of the Gibbs energy G^E is given by Eq. (1):

$$G^E = x_A x_B \sum_{\nu=0}^{n} K_\nu (x_A - x_B)^\nu \quad (1)$$

with

$$K_\nu = A_\nu + B_\nu T + C_\nu T \ln(T) \quad (2)$$

The coefficients A_ν, B_ν and C_ν of Eq. (2) describe the temperature dependence of the parameter K_ν. x_A and x_B are the mole fractions of the limiting compounds. The optimization and calculation of the thermodynamic functions and the phase equilibria were carried out by the 'BINGSS' and 'BINFKT' programs, developed by Lukas et al. [9,10].

4. Binary systems

4.1. The Pb–Sb system

The Pb–Sb system is of the eutectic type with a small range of solubility of the components in the solid state. An assessment of the system was presented by Ashtakala et al. [13]. The system was optimized by Taskinen and Teppo [14] and Ohtani [15]. The thermodynamic properties of the melt were measured using calorimetric [16–20] and EMF methods [21–26]. The excess enthalpies deviate S-shaped from the ideal behaviour [19,20,15], or are only negative over the whole range of concentrations [18,14].

The excess enthalpy values of the Pb–Sb system, used for our calculation, are based on the data of Wittig and Gehring [18] in accordance with the optimization of Taskinen and Teppo [14]. The enthalpies are weakly exothermic with a minimum of ca. -50 J mol^{-1}. The thermodynamic functions are given by one coefficient $C^{H}_{Pb,Sb}$ for the interaction between the elements (Fig. 1).

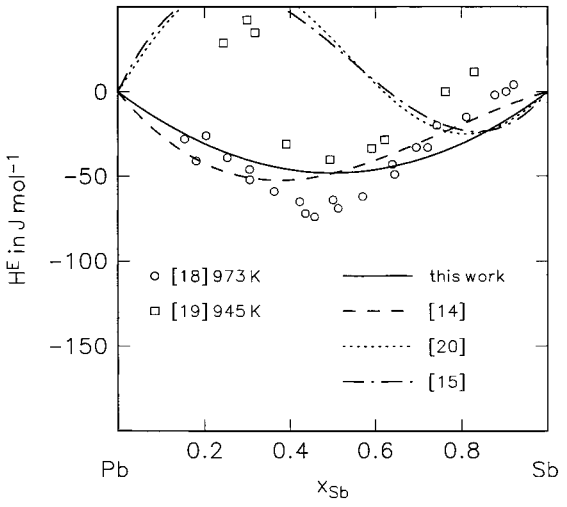

Fig. 1. Experimental (points) and calculated (lines) excess enthalpies of liquid Pb–Sb alloys.

4.2. The Pb–Te system

The Pb–Te system contains the congruent melting compound PbTe with a very small homogeneity range [27]. The system was optimized by different authors [28–31]. The thermodynamic properties of liquid alloys were reported using calorimetric [32,33], vapour-pressure [34], quantitative DTA [35] and EMF methods [36,37].

The excess enthalpies of the Pb–Te system (Fig. 2) are a typical triangular-shaped function of the concentration as known for chemical short-range ordered systems. The enthalpy and entropy of formation of an associate PbTe, ΔH^0_{PbTe} and, ΔS^0_{PbTe}, the interaction parameters $C^{G}_{Pb,PbTe}$ and $C^{G}_{Te,PbTe}$ for the interaction between the associate and the pure components were used for the description of the system. Calculated and experimental excess enthalpies are summarized in Fig. 2.

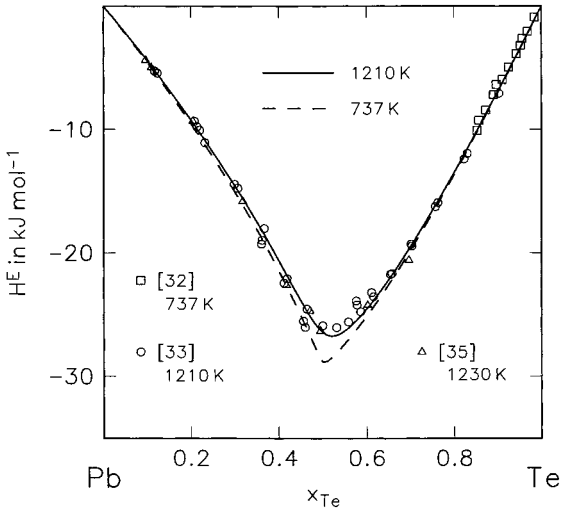

Fig. 2. Experimental (points) and calculated (lines) excess enthalpies of liquid Pb–Te alloys.

4.3. The Sb–Te system

The Sb–Te system contains a congruent melting compound Sb_2Te_3 and two solid phases between Sb

and Sb_2Te_3, δ and γ with a wide homogeneity range [38]. The δ-phase has a melting minimum, whereas the γ-phase melts incongruently. The system was optimized, assessed and calculated by Gosh et al. [39,40]. The thermodynamic properties of liquid alloys were determined by calorimetric [41,42], isopiestic [43] and EMF methods [44,45].

5. Ternary system

Phase diagram investigations in the ternary system were performed by Henger and Peretti [46,47], Reynolds [48] Hirai et al. [49] and Abrikosov et al. [5,6], the latter reported a ternary compound $Pb_2Sb_6Te_{11}$ on the quasi-binary section $PbTe–Sb_2Te_3$. Nasar et al. [50] measured the heat of fusion of this compound.

According to the results of Henger and Peretti [47] the ternary eutectic in the PbTe–Pb–Sb subsystem has a eutectic temperature of T=525.5 K at 88.9 wt% Pb and 11.1 wt% Sb and is identical to that of the Pb–Sb binary eutectic (Table 1).

6. Results

6.1. Calorimetric investigations

6.1.1. The binary Sb–Te system

The results of the calorimetric measurements in the Sb–Te system at 1173 K are given in Table 2. For the addition of Te to liquid Sb–Te alloys, the enthalpies of solution were calculated according to the reaction

$$(1-z)\mathrm{Sb}_{1-x}\mathrm{Te}_x(1,T) + z\mathrm{Te}(s,298\,\mathrm{K}) \overset{\Delta H^{\mathrm{sol}}}{\rightarrow} \mathrm{Sb}_{(1-x)(1-z)}\mathrm{Te}_{x(1-z)+z}(1,T), \quad (3a)$$

The excess enthalpies $H^{\mathrm{E}}_{\mathrm{Sb-Te}}$ were calculated from Eq. (3b)

$$(1-z)(1-x)\mathrm{Sb}(1,T) + [z+(1-z)x]\mathrm{Te}(1,T) \overset{H^{\mathrm{E}}_{\mathrm{Sb-Te}}}{\rightarrow} \mathrm{Sb}_{(1-x)(1-z)}\mathrm{Te}_{x(1-z)+z}(1,T) \quad (3b)$$

similar equations are valid for the addition of Sb to the liquid alloys, namely Eq. (4a) for the enthalpies of solution

Table 1
Coefficients of the association model for the limiting binary systems

System:	Pb–Sb	Pb–Te	Sb–Te
(i,j)	—	1,1	2.3
$\Delta H^0_{\mathrm{A}_i\mathrm{B}_j}$ (kJ/mol)	—	−58.5	−60.9
$\Delta S^0_{\mathrm{A}_i\mathrm{B}_j}$ (J/mol K)	—	−12.6	−51.3
$C^{\mathrm{H}}_{\mathrm{A,B}}$ (kJ/mol)	−0.2	—	−12.0
$C^{\mathrm{S}}_{\mathrm{A,B}}$ (kJ/mol)	—	4.2	—
$C^{\mathrm{H}}_{\mathrm{A},\mathrm{A}_i\mathrm{B}_i}$ (kJ/mol)	—	14.3	−30.8
$C^{\mathrm{S}}_{\mathrm{A},\mathrm{A}_i\mathrm{B}_j}$ (J/mol K)	—	—	—
$C^{\mathrm{H}}_{\mathrm{B},\mathrm{A}_i\mathrm{B}_j}$ (kJ/mol)	—	−13.1	−33.0
$C^{\mathrm{S}}_{\mathrm{B},\mathrm{A}_i\mathrm{B}_j}$ (J/mol K)	—	−8.7	—

Table 2
Enthalpies of solution ΔH^{sol} and binary excess enthalpies $H^{\mathrm{E}}_{\mathrm{Sb-Te}}$ according to the reactions (3) and (4) in the Sb–Te system at 1173 K

n_{Te}/ (mol)	x_{Te}	ΔH^{sol}/ (J/mol)	$H^{\mathrm{E}}_{\mathrm{Sb-Te}}$/ (J/mol)
Starting amount: n_{Sb}=0.015984 mol			
0.001440	0.083	2691	−1104
0.002322	0.191	3867	−2509
0.002452	0.280	3474	−3833
0.003131	0.369	3839	−5198
0.003479	0.445	4028	−6089
0.003489	0.505	3664	−6730
0.003089	0.548	3224	−6928
0.003464	0.589	3140	−7266
Starting amount: n_{Sb}=0.013579 mol			
0.000890	0.062	2010	−817
0.001745	0.163	3683	−1988
0.002142	0.260	3592	−3524
0.003295	0.373	4700	−5280
0.003194	0.453	4160	−6346
n_{Sb}/ (mol)	x_{Te}	ΔH^{sol}/ (J/mol)	$H^{\mathrm{E}}_{\mathrm{Sb-Te}}$/ (J/mol)
Starting amount: n_{Te}=0.017320 mol			
0.000809	0.955	708	−1299
0.001614	0.877	1461	−3409
Starting amount: n_{Te}=0.016505 mol			
0.001013	0.942	647	−1954
0.001521	0.867	1512	−3880
0.002254	0.775	2557	−5675
0.003339	0.670	3845	−7158
0.003220	0.593	4403	−7128
0.002457	0.545	3428	−6770

$$(1-z)\mathrm{Sb}_{1-x}\mathrm{Te}_x(1,T) + z\mathrm{Sb}(s,298\,\mathrm{K}) \overset{\Delta H^{\mathrm{sol}}}{\rightarrow} \mathrm{Sb}_{(1-x)(1-z)+z}\mathrm{Te}_{x(1-z)}(1,T), \quad (4a)$$

and Eq. (4b) for the excess enthalpies

$$[z+(1-z)(1-x)]\mathrm{Sb}(1,T) + (1-z)x\mathrm{Te}(1,T) \overset{H^{\mathrm{E}}_{\mathrm{Sb-Te}}}{\rightarrow} \mathrm{Sb}_{(1-x)(1-z)+z}\mathrm{Te}_{x(1-z)}(1,T). \quad (4b)$$

The exothermic minimum of the excess enthalpies is close to the composition of the congruent melting compound Sb_2Te_3 and is temperature-dependent (Fig. 3). By the assumption of the associate Sb_2Te_3 five parameters had to be used for calculation of the thermodynamic functions, the enthalpy and entropy of formation of the associate, $\Delta H^0_{\mathrm{Sb_2Te_3}}$ and $\Delta S^0_{\mathrm{Sb_2Te_3}}$, and the interaction parameters $C^{\mathrm{G}}_{\mathrm{Sb,Te}}$, $C^{\mathrm{G}}_{\mathrm{Sb,Sb_2Te_3}}$ and $C^{\mathrm{G}}_{\mathrm{Te,Sb_2Te_3}}$. The coefficients for the constituent binaries according to the association model are shown in Table 1. The calculated and experimental excess enthalpies and chemical potentials are illustrated in Figs. 3 and 4.

6.1.2. The ternary Pb–Sb–Te system

The enthalpies of solution ΔH^{sol} (5a, 6a), the excess enthalpies $H^{\mathrm{E}}_{\mathrm{Pb_ySb_{1-x}-Te}}$ (5b, 6b) and the ternary excess enthalpies $H^{\mathrm{E}}_{\mathrm{Pb-Sb-Te}}$ (5c, 6c) are listed in Table 3(a–c) for the sections Pb_ySb_{1-y}–Te with y=0.2, 0.5 and 0.8

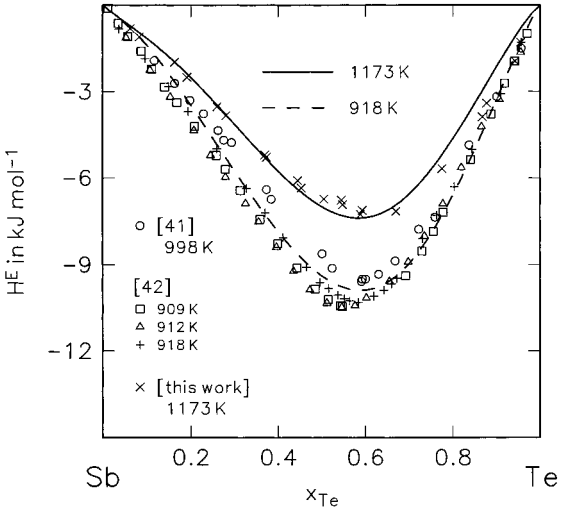

Fig. 3. Experimental (points) and calculated (lines) excess enthalpies of liquid Sb–Te alloys.

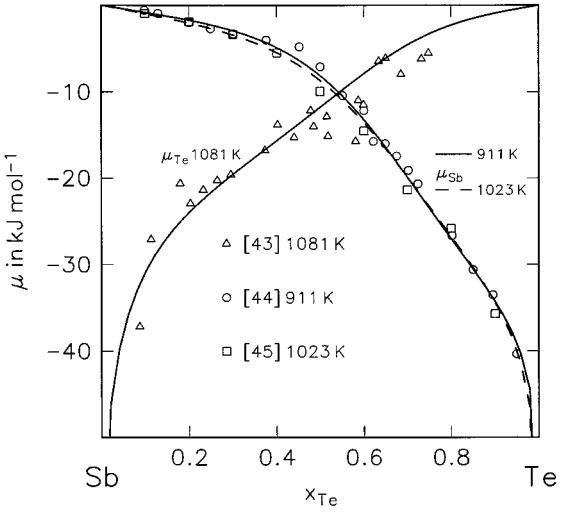

Fig. 4. Experimental (points) and calculated (lines) chemical potentials of liquid Sb–Te alloys.

at 1173 K and in Table 3(d) for the sections $Pb_{0.5}Sb_{0.5}$–Te at 1073 K for the addition of tellurium to liquid alloys according to

$$(1-z)(\mathrm{Pb}_y\mathrm{Sb}_{1-y})_{1-x}\mathrm{Te}_x(1,T) + z\mathrm{Te}(s,298\,\mathrm{K}) \overset{\Delta H^{\mathrm{sol}}}{\rightarrow} (\mathrm{Pb}_y\mathrm{Sb}_{1-y})_{(1-x)(1-z)}\mathrm{Te}_{x(1-z)+z}(1,T), \quad (5a)$$

$$(1-z)(1-x)\mathrm{Pb}_y\mathrm{Sb}_{1-y}(1,T) + [z+(1-z)x] \times \mathrm{Te}(1,T) \overset{H^{\mathrm{E}}_{\mathrm{Pb_ySb_{1-y}-Te}}}{\rightarrow} (\mathrm{Pb}_y\mathrm{Sb}_{1-y})_{(1-x)(1-z)} \times \mathrm{Te}_{x(1-z)+z}(1,T) \quad (5b)$$

and

$$(1-z)(1-x)y\mathrm{Pb}(1,T) + (1-z)(1-x)(1-y) \times \mathrm{Sb}(1,T) + [z+(1-z)x]\mathrm{Te}(1,T) \overset{H^{\mathrm{E}}_{\mathrm{Pb-Sb-Te}}}{\rightarrow} \mathrm{Pb}_{y(1-x)(1-z)}\mathrm{Sb}_{(1-y)(1-x)(1-z)} \times \mathrm{Te}_{x(1-z)+z}(1,T) \quad (5c)$$

and for the addition of $Pb_ySb_{(1-y)}$ to liquid alloys according to

$$(1-z)(\mathrm{Pb}_y\mathrm{Sb}_{1-y})_{1-x}\mathrm{Te}_x(1,T) + z\mathrm{Pb}_y\mathrm{Sb}_{1-y} \times (s,298\,\mathrm{K}) \overset{\Delta H^{\mathrm{sol}}}{\rightarrow} (\mathrm{Pb}_y\mathrm{Sb}_{1-y})_{(1-x)(1-z)+z} \times \mathrm{Te}_{x(1-z)}(1,T), \quad (6a)$$

Table 3
Enthalpies of solution ΔH^{sol}, experimental excess enthalpies $H^{E}_{Pb_ySb_{1-y}-Te}$ and ternary excess enthalpies $H^{E}_{Pb-Sb-Te}$ according to the reactions (5) and (6) along the different sections

n_{Te} (mol)	x_{Te}	ΔH^{sol} (J/mol)	$H^{E}_{Pb_{0.2}Sb_{0.8}-Te}$ (J/mol)	$H^{E}_{Pb-Sb-Te}$ (J/mol)
(a) $Pb_{0.2}Sb_{0.8}$–Te at 1173 K				
Starting amount: $n_{Pb_{0.2}Sb_{0.8}}$=0.016082 mol				
—	0.0	—	0	−19.3
0.001099	0.064	1413	−1423	−1441
0.001997	0.161	2146	−3746	−3763
0.002933	0.273	3116	−6014	−6029
0.003053	0.361	3102	−7563	−7576
0.003702	0.443	3786	−8495	−8505
Starting amount: $n_{Pb_{0.2}Sb_{0.8}}$=0.014477 mol				
—	0.0	—	0	−19.3
0.001005	0.065	1410	−1468	−1496
0.002100	0.177	2496	−4092	−4108
0.002197	0.268	2497	−6066	−6080
0.003067	0.366	3318	−7887	−7900
0.003567	0.452	3901	−8909	−8920
0.002804	0.504	3067	−9243	−9253
0.002150	0.538	2400	−9249	−9258
$n_{Pb_{0.2}Sb_{0.8}}$ (mol)	x_{Te}	ΔH^{sol} (J/mol)	$H^{E}_{Pb_{0.2}Sb_{0.8}-Te}$ (J/mol)	$H^{E}_{Pb-Sb-Te}$ (J/mol)/mol
Starting amount: n_{Te}=0.013031 mol				
—	1.0	—	0	0
0.001213	0.915	280	−3303	−3304
0.001826	0.811	932	−6765	−5254
0.002439	0.704	1991	−9416	−8380
0.002591	0.617	2841	−10574	−10581
0.002496	0.552	3117	−10780	−10788
0.002403	0.501	3382	−10282	−10291
Starting amount: n_{Te}=0.013719 mol				
—	1.0	—	0	0
0.000738	0.949	157	−1985	−1986
0.001160	0.878	610	−4347	−4350
0.001306	0.811	847	−6404	−6408
0.001738	0.735	1276	−8442	−8447
0.001860	0.669	1858	−9624	−9631
0.002332	0.600	2823	−10104	−10112
n_{Te} (mol)	x_{Te}	ΔH^{sol} (J/mol)	$H^{E}_{Pb_{0.5}Sb_{0.5}-Te}$ (J/mol)	$H^{E}_{Pb-Sb-Te}$ (J/mol)
(b) $Pb_{0.5}Sb_{0.5}$–Te				
Starting amount: $n_{Pb_{0.5}Sb_{0.5}}$=0.014626 mol				
—	0.0	—	0	−48.3
0.001477	0.092	834	−3234	−3278
0.002275	0.204	1158	−7165	−7203
0.002300	0.293	1000	−10301	−10335
0.003003	0.382	1328	−13290	−13320
0.003405	0.460	2218	−14975	−15001
0.004354	0.535	3791	−15251	−15273
0.003184	0.578	3033	−14893	−14914

Table 3 (*continued*)

$n_{Pb_{0.5}Sb_{0.5}}$ (mol)	x_{Te}	ΔH^{sol} (J/mol)	$H^{E}_{Pb_{0.5}Sb_{0.5}-Te}$ (J/mol)	$H^{E}_{Pb-Sb-Te}$ (J/mol)
Starting amount: $n_{Pb_{0.5}Sb_{0.5}}$=0.014582 mol				
—	0.0	—	0	−48.3
0.001458	0.091	1132	−2900	−2944
0.002459	0.212	1215	−7194	−7232
0.002788	0.315	1171	−10888	−10921
0.003005	0.400	1490	−13536	−13565
0.003661	0.478	2524	−15047	−15073
0.003886	0.542	3521	−15102	−15124
$n_{Pb_{0.5}Sb_{0.5}}$ (mol)	x_{Te}	ΔH^{sol} (J/mol)	$H^{E}_{Pb_{0.5}Sb_{0.5}-Te}$ (J/mol)	$H^{E}_{Pb-Sb-Te}$ (J/mol)
Starting amount: n_{Te}=0.013308 mol				
—	1.0	—	0	0
0.000706	0.950	−718	−2609	−2611
0.001331	0.867	−673	−6311	−6317
0.001693	0.781	−354	−9767	−9777
0.001868	0.704	−187	−12697	−12711
0.001946	0.638	444	−14571	−14588
0.002094	0.580	1175	−15491	−15511
0.002098	0.531	2002	−15336	−15358
0.002234	0.488	2426	−14728	−14753
Starting amount: n_{Te}=0.013390 mol				
—	1.0	—	0	0
0.000694	0.951	−494	−2343	−2345
0.001384	0.866	−638	−6131	−6137
0.001929	0.770	−307	−9920	−9931
0.001952	0.692	39	−12666	−12681
0.002683	0.608	1120	−14574	−14593
0.002806	0.539	2288	−14880	−14902
n_{Te} (mol)	x_{Te}	ΔH^{sol} (J/mol)	$H^{E}_{Pb_{0.8}Sb_{0.2}-Te}$ (J/mol)	$H^{E}_{Pb-Sb-Te}$ (J/mol)
(c) $Pb_{0.8}Sb_{0.2}$–Te at 1173 K.				
Starting amount: $n_{Pb_{0.8}Sb_{0.2}}$=0.012162 mol				
—	0.0	—	0	−42.5
0.001311	0.097	544	−3771	−3809
0.001703	0.199	120	−8203	−8238
0.001896	0.288	−331	−12548	−12578
0.003193	0.400	−780	−18337	−18363
0.003980	0.498	−267	−22339	−22361
0.004701	0.580	5436	−20477	−20495
0.003723	0.628	4902	−18294	−18310
Starting amount: $n_{Pb_{0.8}Sb_{0.2}}$=0.011072 mol				
—	0.0	—	0	−42.5
0.001382	0.111	653	−4267	−4305
0.001632	0.214	6	−8905	−8938
0.002191	0.320	−406	−14081	−14110
0.002419	0.408	−442	−18438	−18463
0.002861	0.486	833	−21042	−21064

Table 3 (*continued*)

$n_{Pb_{0.8}Sb_{0.2}}$ (mol)	x_{Te}	ΔH^{sol} (J/mol)	$H^{E}_{Pb_{0.8}Sb_{0.2}-Te}$ (J/mol)	$H^{E}_{Pb-Sb-Te}$ (J/mol)
Starting amount: n_{Te}=0.017725 mol				
—	1.0	—	0	0
0.001124	0.940	−1580	−3555	−3558
0.001566	0.868	−1305	−7130	−7135
0.001647	0.803	−1472	−10543	−10552
0.001851	0.741	−1366	−13658	−13669
0.002351	0.675	−1389	−16790	−16804
0.002591	0.614	−919	−19177	−19194
0.002827	0.559	93	−20330	−20348
Starting amount: n_{Te}=0.013284 mol				
—	1.0	—	0	0
0.000569	0.959	−1226	−2586	−2588
0.000970	0.896	−1343	−5928	−5932
0.001320	0.823	−1747	−9900	−9907
0.001789	0.741	−1909	−14127	−14138
0.002807	0.641	−2163	−18863	−18878
0.003185	0.555	−703	−21466	−21485
0.003223	0.489	1889	−20963	−20985

n_{Te} (mol)	x_{Te}	ΔH^{sol} (J/mol)	$H^{E}_{Pb_{0.5}Sb_{0.5}-Te}$ (J/mol)	$H^{E}_{Pb-Sb-Te}$ (J/mol)
(d) $Pb_{0.5}Sb_{0.5}$—Te at 1073 K				
Starting amount: $n_{Pb_{0.5}Sb_{0.5}}$=0.015212 mol				
—	0.0	—	0	−48.3
0.001261	0.077	512	−2736	−2781
0.001716	0.164	460	−6022	−6062
0.002067	0.249	−4178	−13914	−13950
0.002330	0.326	−4561	−21416	−21448
0.002745	0.399	3148	−20544	−20573
0.003312	0.469	5949	−17125	−17151
0.003535	0.527	2585	−17320	−17343
0.003347	0.572	2931	−16755	−16775
Starting amount: $n_{Pb_{0.5}Sb_{0.5}}$=0.017957 mol				
—	0.0	—	0	−48.3
0.001193	0.062	405	−2238	−2283
0.001676	0.138	354	−5118	−5160
0.001990	0.213	−940	−9312	−9350
0.002593	0.293	−6557	−19249	−19283
0.002772	0.363	−1696	−23225	−23256
0.002910	0.422	4208	−20814	−20842
0.003025	0.474	4359	−18372	−18397

$n_{Pb_{0.5}Sb_{0.5}}$ (mol)	x_{Te}	ΔH^{sol} (J/mol)	$H^{E}_{Pb_{0.5}Sb_{0.5}-Te}$ (J/mol)	$H^{E}_{Pb-Sb-Te}$ (J/mol)
Starting amount: n_{Te}=0.015361 mol				
—	1.0	—	0	0
0.000916	0.944	−889	−2834	−2837
0.001359	0.871	−667	−5945	−5952
0.001955	0.784	−956	−9757	−9768
0.002000	0.711	−598	−12652	−12666

Table 3 (*continued*)

0.002293	0.643	−249	−15004	−15022
0.002515	0.582	530	−16337	−16357
Starting amount: n_{Te}=0.016371 mol				
—	1.0	—	0	0
0.000912	0.947	−881	−2704	−2707
0.001516	0.871	−1507	−6779	−6786
0.002068	0.785	−972	−10505	−10515
0.002379	0.704	−938	−13904	−13918
0.002477	0.636	−751	−16644	−16662
0.002532	0.579	513	−17736	−17757
0.002768	0.528	1275	−17963	−17985
0.003743	0.471	1290	−18459	−18484

$$[z+(1-z)(1-x)]\mathrm{Pb}_y\mathrm{Sb}_{1-y}(1,T)+(1-z)x \times \mathrm{Te}(1,T) \overset{H^{E}_{\mathrm{Pb}_y\mathrm{Sb}_{1-y}-\mathrm{Te}}}{\rightarrow} (\mathrm{Pb}_y\mathrm{Sb}_{1-y})_{(1-x)(1-z)+z} \times \mathrm{Te}_{x(1-z)}(1,T) \quad (6b)$$

and

$$[z+(1-z)(1-x)]y\mathrm{Pb}(1,T) + [z+(1-z)(1-x)](1-y)\mathrm{Sb}(1,T) + (1-z)x\mathrm{Te}(1,T) \overset{H^{E}_{\mathrm{Pb-Sb-Te}}}{\rightarrow} \mathrm{Pb}_{y[(1-x)(1-z)+z]} \times \mathrm{Sb}_{(1-y)[(1-x)(1-z)+z]}\mathrm{Te}_{x(1-z)}(1,T). \quad (6c)$$

The excess enthalpies $H^{E}_{Pb-Sb-Te}$ of Eqs. (5c) and (6c) were calculated using the optimized thermodynamic data of the binary Pb–Sb system [14]. In a first step, the calculation was carried out only using the coefficients of the constituent binaries (Fig. 5(a–d), dashed lines). The deviation from the experimental values was significant, therefore ternary interactions were assumed; i.e. between a binary associate and the third component, PbTe↔Sb and Sb_2Te_3↔Pb, and between both associates, PbTe↔Sb_2Te_3 (Fig. 6). The thermodynamic functions were then determined from the following equation and are plotted in Fig. 5(a–d) (solid lines).

$$H^{E}_{Pb-Sb-Te} = \frac{n_{Pb}n_{Sb}}{n}C^{H}_{Pb,Sb} + n_{PbTe}\Delta H^{0}_{PbTe} + \frac{n_{Pb}n_{PbTe}}{n}C^{H}_{Pb,PbTe} + \frac{n_{Te}n_{PbTe}}{n}C^{H}_{Te,PbTe} + n_{Sb_2Te_3}\Delta H^{0}_{Sb_2Te_3} + \frac{n_{Sb}n_{Sb_2Te_3}}{n}C^{H}_{Sb,Sb_2Te_3} + \frac{n_{Te}n_{Sb_2Te_3}}{n}C^{H}_{Te,Sb_2Te_3} + \frac{n_{Sb}n_{Te}}{n}C^{H}_{Sb,Te} + \frac{n_{Sb}n_{PbTe}}{n}C^{H}_{Sb,PbTe} + \frac{n_{Pb}n_{Sb_2Te_3}}{n}C^{H}_{Pb,Sb_2Te_3} + \frac{n_{PbTe}n_{Sb_2Te_3}}{n}C^{H}_{PbTe,Sb_2Te_3}. \quad (7)$$

The coefficients of the last three terms were fitted by a numerical optimization procedure using the least-squares method [51]. The ternary coefficients are summarized in Table 4. All interactions used for the calculation are displayed in Fig. 6. Fig. 7 presents the isoenthalpic curves in a projection onto the Gibbs triangle. The minima in the enthalpy surface are forming a valley stretching from PbTe to Sb_2Te_3.

The curves of the ternary excess enthalpies along the section $Pb_{0.5}Sb_{0.5}$–Te have a minimum of −16.6 kJ mol^{-1} and 56 mol% at 1073 K and of −15.5 kJ mol^{-1} and 55 mol% at 1173 K. The deviation from the experimental excess enthalpies at 1073 K between 20 and 50 mol% Te is caused by the primary crystallisation of PbTe.

6.2. Phase diagram investigations

6.2.1. The quasi-binary sections PbTe–Sb_2Te_3 and PbTe–Sb

For the optimization of the quasi-binary sections, we used our own and other available phase diagram data [5,6,46–49]. The ternary compound reported by Abrikosov et al. [5] was not considered because various attempt for its preparation failed. The calculated excess enthalpies for the ternary system were

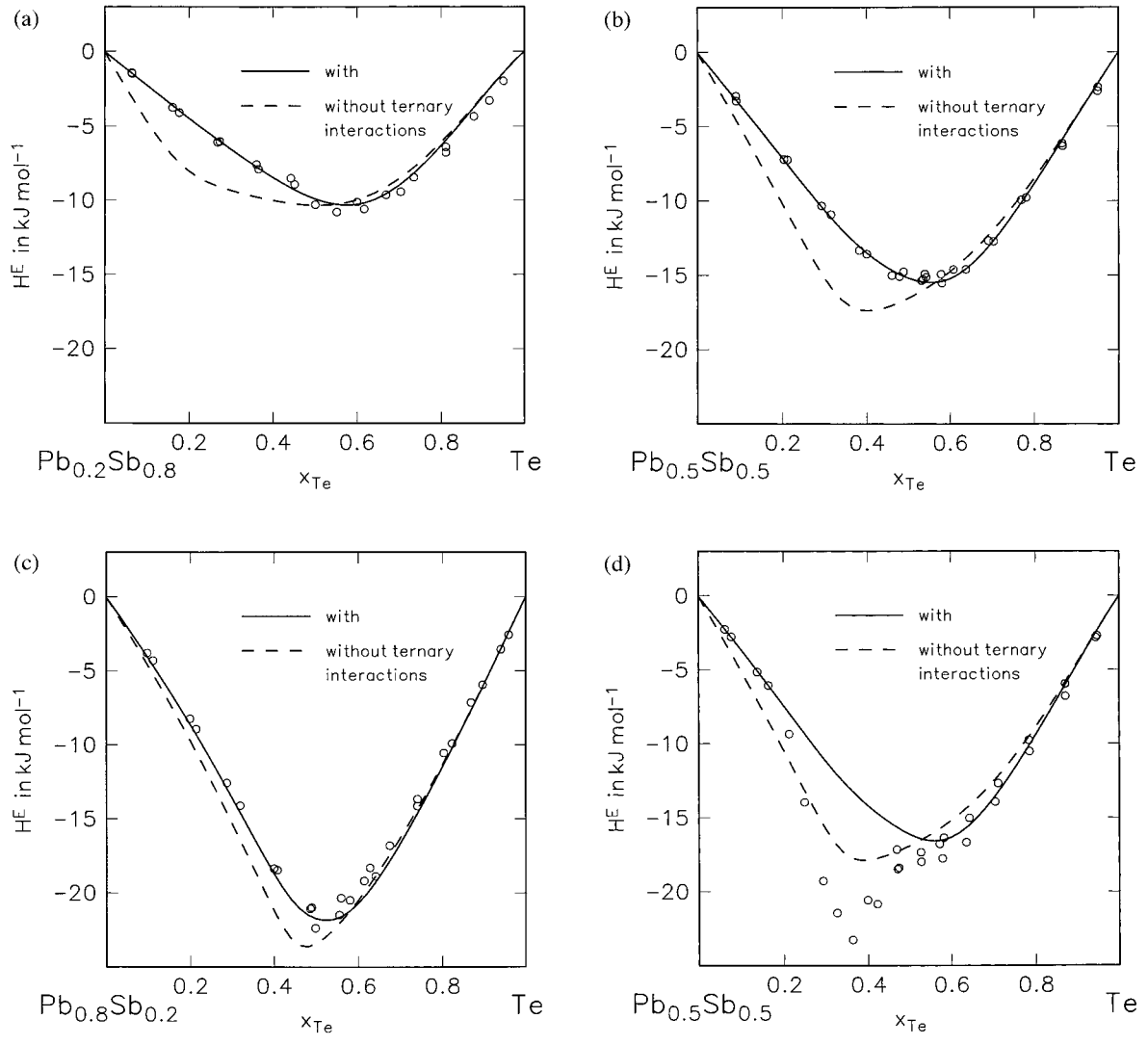

Fig. 5. Experimental and calculated excess enthalpies of liquid Pb–Sb–Te alloys along the sections Pb_ySb_{1-y}–Te. (- - -) Calculated with only the binary coefficients in Table 1; (———) calculated with additional ternary coefficients in Table 4: (a) $Pb_{0.2}Sb_{0.8}$–Te section at 1173 K, (b) $Pb_{0.5}Sb_{0.5}$–Te section at 1173 K, (c) $Pb_{0.8}Sb_{0.2}$–Te section at 1173 K, and (d) $Pb_{0.5}Sb_{0.5}$–Te section at 1073 K.

Table 4
Coefficients of the association model of the ternary interactions in the Pb–Sb–Te system

$C^{H}_{Sb,PbTe}$/ (kJ/mol)	C^{H}_{Pb,Sb_2Te_3}/ (kJ/mol)	C^{H}_{PbTe,Sb_2Te_3}/ (kJ/mol)
22.5	−3.0	−33.6

transformed to values of the quasi-binary section according to

$$H^{E}_{PbTe-Sb} = \frac{H^{E}_{Pb-Sb-Te} - (n_{PbTe}H^{E}_{PbTe})}{n_{PbTe} + n_{Sb}} \quad (8)$$

for PbTe–Sb and

$$H^{E}_{PbTe-Sb_2Te_3} = \frac{H^{E}_{Pb-Sb-Te} - (n_{PbTe}H^{E}_{PbTe} + n_{Sb_2Te_3}H^{E}_{Sb_2Te_3})}{n_{PbTe} + n_{Sb_2Te_3}} \quad (9)$$

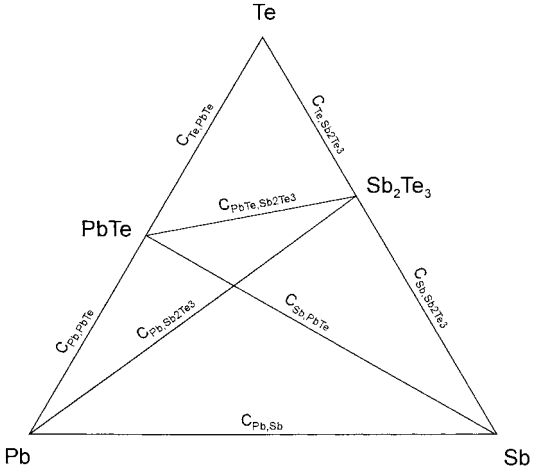

Fig. 6. Coefficients of the association model projected on the Gibbs triangle of the Pb–Sb–Te system.

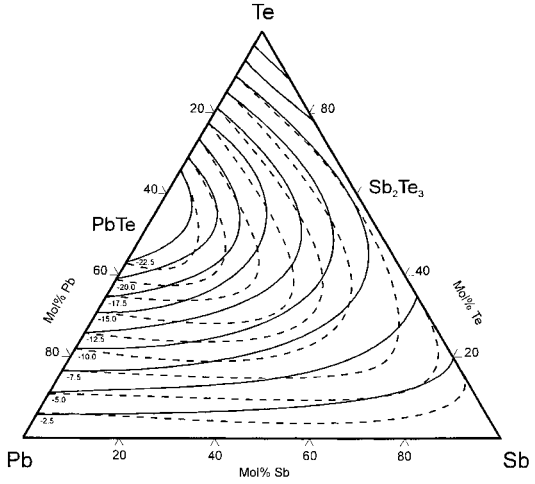

Fig. 7. Calculated isoenthalpic lines projected on the Gibbs triangle of the Pb–Sb–Te system in kJ mol^{-1}. (- - -) Calculated with only the binary coefficients in Table 1; (———) calculated with additional ternary coefficients in Table 4.

for PbTe–Sb_2Te_3. The results of DTA measurements are given in Table 5(a) and (b).

The coefficients in Eq. (10), which describe the temperature dependence of the Gibbs enthalpy of the pure components

$$G_i(T) - H_i^{SER}(298.15\,K) = A + BT + CT\ln(T) + DT^2 \ldots \quad (10)$$

Table 5
Experimental liquidus and solidus temperatures on the quasi-binary PbTe–Sb_2Te_3

$x_{Sb_2Te_3}$	$T_{solidus}$/K	$T_{liquidus}$/K
(a)		
0.043	864	1183
0.091	864	1154
0.146	865	1131
0.211	864	1091
0.286	866	1048
0.375	862	1000
0.483	865	947
0.615	864	—
0.783	864	883

(b)		
x_{Sb}	$T_{solidus}$/K	$T_{liquidus}$/K
0	—	1201
0.095	880	1184
0.182	881	1174
0.261	880	1159
0.333	880	1143
0.400	877	1109
0.519	880	1113
0.571	882	1098
0.621	876	1090
0.667	883	1077
0.710	878	1062
0.750	882	1049
0.788	881	1046
0.824	881	1025
0.857	882	1013
0.889	881	966
0.919	880	913
0.947	882	885
0.974	881	889
0.974	877	901

are presented in Table 6, those of Sb were taken from the SGTE datafile [52], those of PbTe and Sb_2Te_3 were derived from the values given by Barin [3].

The phase diagrams and the excess enthalpy curves calculated with the adjusted set of coefficients (Table 7(a) and (b)) are shown in Figs. 8 and 9 for the PbTe–Sb system and in Figs. 10 and 11 for the PbTe–Sb_2Te_3 system. The homogeneity ranges of PbTe and Sb_2Te_3 (dashed lines in Figs. 10 and 11) were approximated, because sufficient data were not available.

Table 6
Coefficients for the description of the Gibbs enthalpy of the limiting phases for the quasi-binary sections in the Pb–Sb–Te system.

Phase	Temperature range/ K	$G_i(T) - H_i^{SER}$ (298.15 K)
Sb (solid)	298.15<T<903.9	$-9242.858+156.154689T-30.5130752T\ln(T)$ $+7.748768\times10^{-3}T^2+100625T^{-1}-(3.0034150\times10^{-6})T^3$
	903.9<T<3200	$-11738.671+169.485713T-31.3800T\ln(T)$ $(1.310442\times10^{27})T^{-9}$
Sb (liquid)	298.15<T<903.9	$10579.737+134.234092T-30.5130752T\ln(T)$ $+7.748768\times10^{-3}T^2$ $+100625T^{-1}-(3.003415\times10^{-6})T^3+(1.73785\times10^{-21})T^7$
	903.9<T<3200	$8175.311+147.458958T-31.38T\ln(T)$
PbTe (solid)	298.15<T<1700	$-14563.5+209.243T-47.1693T\ln(T)-5.64593\times10^{-3}T^2$
PbTe (liquid)	298.15<T<1700	$32168.22+274.01T-62.77T\ln(T)$
Sb_2Te_3 (solid)	298.15<T<1700	$-36004.3+525.12593T-112.831568T\ln(T)-2.66148\times10^{-2}T^2$
Sb_2Te_3 (liquid)	298.15<T<1700	$9159.62+1021.57T-196.856T\ln(T)$

Table 7
Coefficients, according to the Redlich–Kister polynomial description of the quasibinary section PbTe–Sb

Phase	ν	A_ν/ (J/mol)	B_ν/ (J/mol·K)
(a) PbTe–Sb			
	0	38251.58	−30.50960
Liquid	1	−2492.94	4.85275
	2	−6386.29	
(PbTe)	0	25000	
(b) PbTe–Sb_2Te_3			
	0	5694.83	−27.55303
Liquid	1	1350.32	−16.17402
	2	−2175.72	
(PbTe)	0	16773.10	
(Sb_2Te_3)	0	22000	

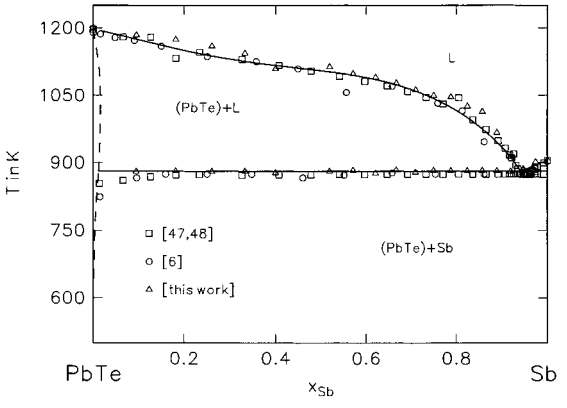

Fig. 8. Calculated phase equilibria in the quasi-binary PbTe–Sb system.

7. The ternary Pb–Sb–Te system

Due to the short annealing time, we did not observe the δ- and γ-Phase in the Sb–Sb_2Te_3 subsystem. The ternary system is characterized by a broad primary crystallisation range of PbTe and divided into three subternaries by the two quasi-binaries PbTe–Sb_2Te_3 and PbTe–Sb. The liquidus surface of the ternary system was constructed from the results of our phase diagram investigations[2] and is shown in Fig. 12. The alloys on the quasi-binary PbTe–Sb have the highest melting points which decrease smoothly from PbTe into the direction of the Pb–Sb and Sb–Te binaries, respectively.

The ternary eutectics are found for the PbTe–Sb_2Te_3–Te subsystem at the composition x_{Pb}=0.92, x_{Sb}=0.05, x_{Te}=0.08 (Δx=0.02) with a eutectic temperature of T=672±3 K and degenerated for PbTe–Pb–Sb with a temperature of T=527±3 K, very close to that in the Pb–Sb binary. The agreement between our results and those given by Henger and Peretti [47] is acceptable.

[2]Data available from the corresponding author.

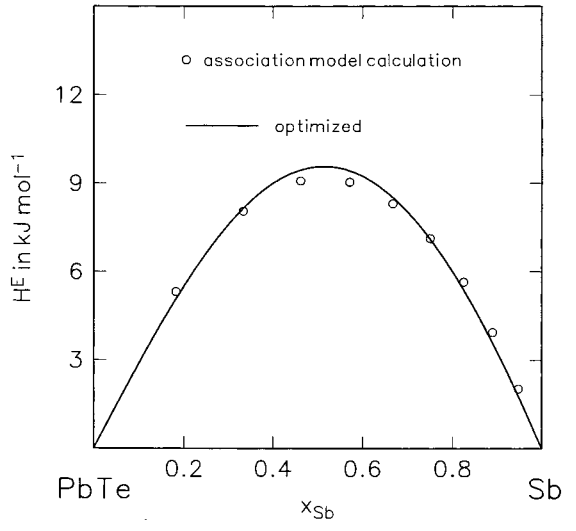

Fig. 9. Calculated (points) and optimized (full line) excess enthalpies in the quasi-binary PbTe–Sb system.

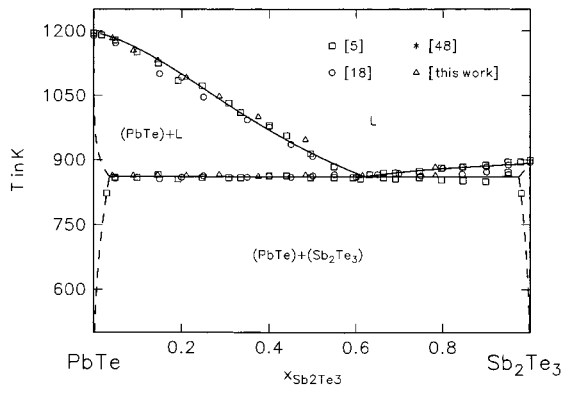

Fig. 10. Calculated phase equilibria in the quasi-binary PbTe–Sb system.

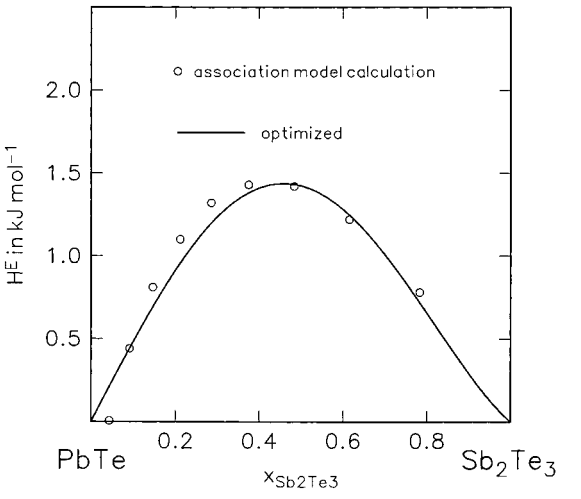

Fig. 11. Calculated (points) and optimized (full line) excess enthalpies in the quasi-binary PbTe–Sb_2Te_3 system.

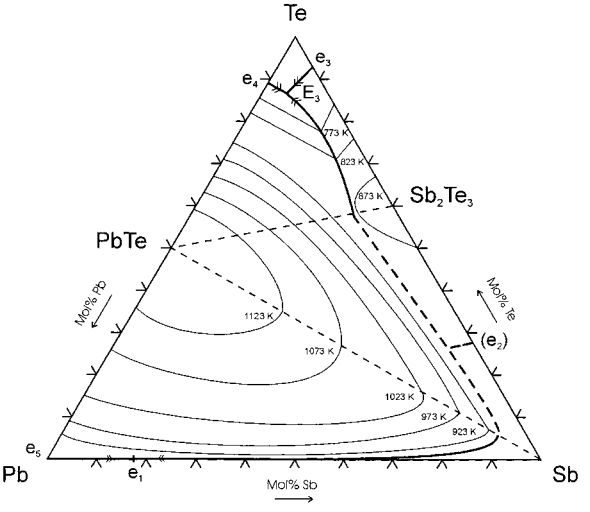

Fig. 12. Liquidus surface of the system Pb–Sb–Te.

8. Discussion

Though both binary tellurium systems contain associates, their thermodynamic behaviours differ:

The excess enthalpy curve of the Pb–Te system is a sharp triangular-shaped function of concentration and independent of the temperature (Fig. 2). The interaction between metallic Pb and the associate PbTe is repulsive, which is indicated by a positive interaction parameter $C^{H}_{Pb,PbTe}$. The tendency for the formation of associates in the system is strong ($K_{PbTe}\approx100$ at 1173 K). Interaction between the pure components Pb and Te can thus be neglected.

The excess enthalpy curve of the Sb–Te system is a more parabolic function of concentration and is temperature-dependent (Fig. 3). The interactions between Sb and Sb_2Te_3 are attractive as revealed by a negative interaction parameter C^{H}_{Sb,Sb_2Te_3}. This assumption is confirmed by wide ranges of solid solutions between Sb and Sb_2Te_3. The amount of associates formed is much lower than in the Pb–Te system ($K_{Sb_2Te_3} \approx 1$ at

1173 K). An interaction parameter between the pure components has to be applied.

The interactions between Te and the associates, Te↔PbTe and Te↔Sb_2Te_3, are weakly attractive, which is indicated by a negative sign of $C^{H}_{Te,PbTe}$ and C^{H}_{Te,Sb_2Te_3} due to the tendency to form polytellurides.

For an analytical description of the Pb–Sb–Te system, three additional interaction parameters, $C^{H}_{Sb,PbTe}$ and C^{H}_{Pb,Sb_2Te_3}, C^{H}_{PbTe,Sb_2Te_3}, had to be used. If the experimental data were fitted only with binary parameters, the calculated values, in some parts of the system, are more exothermic than the experimental. The maxima of these deviations are following a line stretching from PbTe to Sb (Fig. 7). These deviations are compensated by the assumption of ternary interactions because of the positive coefficient $C^{H}_{Sb,PbTe}$. This endothermic reaction is also revealed by very low solid solubility of Sb in PbTe. Using these ternary interaction parameters, the experimental and calculated excess enthalpies are in good agreement.

Nasar et al. [50] measured the heat of fusion $Pb_2Sb_6Te_{11}$ with ΔH_f=19.3 kJ g^{-1} $atom^{-1}$. However, in reality this composition is a eutectic alloy at 60 mol% Sb_2Te_3 in the PbTe–Sb_2Te_3 system. The value for the eutectic reaction calculated in this work is 21.6 kJ g^{-1} $atom^{-1}$, which is in a reasonable agreement with the experimental value.

9. Conclusion

As in case of the results of the Ge–Sn–Te system [8], the thermodynamic behaviour of the ternary Pb–Sb–Te system can be described by means of the association model. By measuring the thermodynamic data, a set of consistent coefficients was obtained. They could be related to chemical effects, which makes the association model more transparent than polynomial functions. The coefficients of the ternary systems can be applied in future to higher ordered multicomponent systems and can provide information without additional measurements.

Acknowledgements

The authors express their gratitude to the DAAD and the ''Fonds der Chemie'' for their support.

References

[1] C. Wagner, Thermodynamics of Alloys, Addison-Wesley, Reading, MA, 1952.
[2] B. Gather, R. Blachnik, J. Chem. Thermodyn. 16 (1984) 487–495.
[3] I. Barin, Thermochemical Data of Pure Substances, Part I+II, VCH, Weinheim, 1989.
[4] B. Gather, R. Blachnik, J. Less-Common Met. 48 (1976) 205–212.
[5] N.Kh. Abrikosov, E.J. Elagina, M.A. Popova, Izv. Akad. Nauk SSSR, Neorg. Mater. 1 (1965) 2151–2154.
[6] N.Kh. Abrikosov, E.V. Skudnova, L.V. Poretskaya, T.A. Osipova, Inorg. Mater. 5 (1969) 630–633.
[7] F. Sommer, Z. Metallkd. 73 (1982) 72–85.
[8] A. Schlieper, R. Blachnik, Z. Metallkd. 89 (1998) 3.
[9] H.L. Lukas, E.Th. Henig, B. Zimmermann, CALPHAD 1 (1977) 225–236.
[10] H.L. Lukas, S.G. Fries, J. Phase Equilibria 13 (1992) 532–541.
[11] O. Redlich, A. Kister, Indust. Eng. Chem. 40 (1948) 345–348.
[12] H.L. Lukas, S.G. Fries, U. Kattner, J. Weiss, BINGSS, BINFKT, TERGSS, TERFKT, Reference Manual, Version 95-1, 1995.
[13] S. Ashtakala, A.D. Pelton, C.W. Bale, Bull. Alloy Phase Diagrams 2 (1981) 86–89.
[14] P. Taskinen, O. Teppo, Scand. J. Metallurgy 21 (1992) 98–103.
[15] H. Ohtani, K. Okuda, K. Ishida, J. Phase Equilibria 16 (1995) 416–429.
[16] M. Kawakami, Sci. Rept. Tohoku Imp. Univ. Ser. 1, 19 (1930) 521–549.
[17] W. Oelsen, F. Johannsen, A. Podgornik, Z. Erzbergbau Metallhüttenwesen 9 (1956) 459–469.
[18] F.E. Wittig, E. Gehring, Ber. Bunsenges. 71 (1967) 372–376.
[19] A. Yazawa, T. Kawashima, T. Itagaki, Nippon Kinzoku Gakkaishi 32 (1968) 1288–1293.
[20] M. Azzaoui, M. Notin, J. Hertz, Z. Metallkd. 84 (1993) 545–551.
[21] H. Seltz, B.J. DeWitt, J. Amer. Chem. Soc. 61 (1939) 2594–2597.
[22] J.F. Elliott, J. Chapman, J. Amer. Chem. Soc. 73 (1951) 2682–2693.
[23] E. Schürmann, H. Träger, Arch. Eisenhüttenwesen 6 (1961) 397–408.
[24] K. Okajima, H. Sakao, Trans. Jpn. Inst. Met. 11 (1970) 180–184.
[25] Z. Moser, K.L. Komarek, A. Mikula, Z. Metallkd. 67 (1976) 303–306.
[26] E. Sugimoto, Z. Kozuka, S. Kuwata, Nippon Kogyo Kaishi 98 (1982) 429–435.
[27] J.-C. Lin, K.-C. Hsieh, R.C. Sharma, Y.A. Chang, Bull. Alloy Phase Diagrams 10 (1989) 340–347.
[28] M.T. Clavaguera-Mora, N. Calvaguera, J. Onrubia, R. Cohen-Adad, J. Less-Common Met. 119 (1986) 277–289.
[29] U. Kattner, H.L. Lukas, G. Petzow, CALPHAD 10 (1986) 103–115.

[30] T. Leo Ngai, D. Marshall, R.C. Sharma, Y.A. Chang, Monatsh. Chem. 118 (1987) 277–300.
[31] V.L. Kuznetsov, V.P. Zlomanov, Inorg. Mater. 25 (1989) 923–927.
[32] R. Castanet, Y. Claire, M. Laffitte, High Temp.-High Press. 4 (1972) 343–351.
[33] R. Blachnik, B. Gather, J. Less-Common Metals 92 (1983) 207–213.
[34] B. Predel, J. Piehl, M.J. Pool, Z. Metallkd. 66 (1975) 347–352.
[35] S.A. Al'fer, L.A. Mechkovskii, A.A. Vecher, Russ. J. Phys. Chem. 56 (1982) 1597–1598.
[36] B. Fuglewicz, Pol. J. Chem. 58 (1984) 983–989.
[37] N. Moniri, C. Petot, Thermochim. Acta 77 (1984) 151–166.
[38] T.B. Massalski, Binary Alloy Phase Diagrams, 2nd edn., ASM, Metals Park, OH, 1990.
[39] G. Gosh, H.L. Lukas, L. Delay, Z. Metallkd. 80 (1989) 731–736.
[40] G. Gosh, J. Phase Equilibria 15 (1994) 349–360.
[41] T. Maekawa, T. Yokokawa, K. Niwa, J. Chem. Thermodyn. 4 (1972) 153–157.
[42] Y. Feutelais, B. Legendre, G. Morgant, J. Therm. Anal. 34 (1988) 1093–1100.
[43] G. Bolte, Diplomarbeit, Technische Universität Clausthal, 1975.
[44] Y. Feutelais, B. Legendre, S. Misra, T.J. Anderson, J. Phase Equilibria 15 (1994) 171–177.
[45] B. Onderka, K. Fitzner, Z. Metallkd. 86 (1995) 313–318.
[46] G.W. Henger, E.A. Peretti, J. Chem. Eng. Data 10 (1965) 16–18.
[47] G.W. Henger, E.A. Peretti, J. Less-Common Metals 8 (1965) 124–135.
[48] R.A. Reynolds, J. Electrochem. Soc. 114 (1967) 526–529.
[49] T. Hirai, Y. Takeda, K. Kurata, J. Less-Common Metals 13 (1967) 352–356.
[50] A. Nasar, T.K.S.P. Gupta, M. Shamsuddin, Proc. Natl. Symp. Therm. Anal., 9th, 1993, pp. 553–556.
[51] A. Schlieper, Thermodynamische Untersuchungen in Tellurhaltigen Mehrkomponentensystemen, Dissertation, Universität Osnabrück, 1996.
[52] A.T. Dinsdale, CALPHAD 15 (1991) 319–427.